Enhancement of Rheological Properties of Nano-Fe_2O_3-Modified Drilling Fluids

Abdoulaye Seyni Mahamadou[1]* and Gu Jun[1]

[1]Department of Petroleum Engineering, Faculty of Earth Resources, China University of Geosciences

Summary

In this study, we explore the potential of using nanoparticles (NPs) to enhance the properties of water-based drilling fluids (WBDFs). Specifically, we investigate the effects of nano-Fe_2O_3 on the rheological behavior of drilling fluid muds under high-temperature and high-pressure (HTHP) conditions to determine the optimal concentration of Fe_2O_3 NPs to maintain consistent rheology and improve drilling fluid systems. Results show that as temperature increases, the rheological properties of water-based muds (WBMs) decrease, leading to compromised structural integrity. To address this issue, nano-Fe_2O_3 is introduced into the system. We prepared and evaluated six WBM formulations with varying weight percentages of Fe_2O_3 NPs, and found that an optimal NP concentration of 2.5 g wt% resulted in a 13.8% reduction in American Petroleum Institute (API) filtrate volume and a 40% reduction in filter-cake thickness. Under conditions of 300°F temperature and 10,000 psi pressure, consistent reductions were observed in the rheological properties of plastic viscosity (PV), yield point (YP), and gel strength with the addition of Fe_2O_3 NPs. The YP-PV span was measured at 2.7, and the yield strength was determined to be 11 lb/100 ft^2. Regarding fluid loss, Drilling Mudcake A containing 0.5 wt% NPs experienced a loss of 6 mL of fluid after 30 minutes, whereas Mudcake E containing 3 wt% NPs exhibited a fluid loss of 5.1 mL in the API filter press test. According to the Bingham plastic model, Muds E and F, containing 2.5 wt% and 3 wt% NPs, respectively, displayed the maximum shear stress vs. shear rate. This highlights the efficacy of nano-Fe_2O_3 in adjusting the properties of drilling fluids, presenting opportunities for enhanced performance and efficiency in drilling operations.

Introduction

The superior itemizing and planning design of the exhausting fluids system is the best approach to showing the objective significance of the hydrocarbon vault. Drilling fluids (e.g., oil-based mud, WBDF) are primarily used to drain oil and gas wells. They have demonstrated a sophisticated method of handling the acting of rheological characteristics under various crippling conditions (Baba Hamed and Belhadri 2009; Livescu 2012). WBDFs are widely used among these weakening liquids and are regarded as unassuming and inoffensive to the biological structure (Christiansen 1991; Mao et al. 2015; Rodrigues et al. 2006; Sadeghalvaad and Sabbaghi 2015; Tehrani et al. 2009). Nevertheless, it has also been declared that massive extension, restricted application, and polymer-added material may give rise to concerns regarding unstable rheological characteristics in downhole circumstances of HTHP (Abdo and Haneef 2013; Abdo et al. 2014; Mao et al. 2015).

The oil and gas industry generally views the increase of potassium chloride in WBDFs as a means of better hydration blockage and control over rheological qualities, particularly in shale (Khodja et al. 2010). At high temperatures and high pungency circumstances, the rheology and filtration characteristics of exhausting muds with water-dissolvable polymers alter the working conditions (Vermolen et al. 2011). NPs have been added to water-setup mud works to address the viscoelastic and thixotropic properties of WBM rheological congruity of penetrating muds (Aadnoy and Chenevert 1987; Coussot et al. 2004; Le Guen et al. 2009).

Riley et al. (2012) assessed the use of silica nanomaterial in water-based fluids to further develop restraint of shale materials and contrasted it and an engineered-based mud, which is regularly utilized for wellbore soundness worries in shale arrangements. The example with 3 wt% of silica delivered a penetrability decrease of 20.1%, more prominent than the base example without silica, showing its capacity to fit and seal miniature pores and miniature breaks. Abduo et al. (2016) tried bentonite with molecule size between 4 nm and 9 nm as an added substance to WBDFs and contrasted the outcomes and programming interface bentonite properties and an example with neighborhood bentonite not at a nanosize. The generally rheological properties, such as apparent viscosity, PV, and YP, diminished because of the expansion of bentonite with nanosize distance across, as the strong substance of the liquid was diminished.

When it comes to controlling the rheological properties of depleting fluids, Mao et al. and Jain et al. recommend using nanocomposites as an alternative to soils and polymers (Mao et al. 2015; Jain et al. 2015). Nanocomposites are used to fight against the difficulties brought on by the intense heat and pressure of the more important course of action due to the warm defilement of the mud sections when entering mud. To modify the rheological properties and shale hindrance of WBMs, harmful mud additives, such as multiwalled carbon nanotubes, graphene nanoplatelets, and nanosilica, were added by Ismail et al. The results of that study showed that graphene nanoplatelets can be used as an overlay option to improve the execution of WBM (Ismail et al. 2016).

The use of NPs in the oil business will permit penetrating designers to change the rheology of the boring liquid by changing the arrangement (Abdo and Haneef 2012). NPs can work on the rheological qualities of drilling fluids by utilizing different instruments that fundamentally rely upon the consistent period of penetrating liquids and the attributes of the NPs (Brady and Brady 1983; Jain et al. 2015; Taraghikhah et al. 2015). This advancement in the consistency of nanofluids can be assessed by utilizing homogeneous strong liquid connection models (Singh et al. 2011) and fixed modified emulsion drilling fluids at HTHP conditions with soil and silica NPs (László et al. 2001). Those authors found that, either separately or in combination, nanosoil and nanosilica can immobilize or modify emulsions that enter fluids. Both thickness and yield strength are improved when the additional Fe_2O_3 particles in the bentonite liquid become more centrally distributed (Nasser et al. 2013).

The progress of drilling mud is because they increment oil recuperation and decline the time expected to get the principal oil (Nagre et al. 2014). The rheological elements of a drilling mud can be prepared by many variables during the boring activity, for example,

*Corresponding author; email: zaroumey2005@yahoo.fr

Original SPE manuscript received for review 23 January 2024. Revised manuscript received for review 21 July 2024. Paper (SPE 223105) peer approved 7 August 2024.

temperature, pressure that is a component of boring profundity, and impurities (Khoshakhlagh et al. 2012). According to some theories, nano-Fe_2O_3 can significantly affect compressive strength, flexural strength, and controllable splitting strength by up to 5% at particular easing times (Rashad 2013). The cementitious material's convenience, setting time, mechanical strength, water retention, and durability were all improved by the nanoiron oxide Fe_2O_3 (Nelson et al. 1990). The gel structure gives adequate consistency to allow for development in the water content in the substantial without having free water (Akhtarmanesh et al. 2013). Mahmoud et al. (2019) found that to lessen porousness and liquid intrusion, the base colloidal silica NP fixation should be 10 wt%, and a superior stopping execution was noted with the 35 nm measured NPs when contrasted with the 50 nm NPs. Then again, water-based liquids are widely utilized for boring applications because of their minimal expense, simplicity to deal with, lack of imperative removal, and because they are harmless to the ecosystem contrasted with oil-based fluids (Li et al. 2019).

A polyacrylamide (PAM)-based copolymer was used to upgrade the shale security of delicate shale developments in the penetrating system (Aramendiz and Imqam 2019). A few NPs were utilized to upgrade the shale-restraint properties, such as nanosilica (Ma et al. 2020), multivalued carbon nanotubes (Rana et al. 2020), graphene (Bayat and Shams 2019; Mady et al. 2020), and Fe_2O_3 (Du et al. 2019). Nanomaterial is utilized in the definition of concrete to build its solidarity and strength (Esmaeili et al. 2011; Sikora et al. 2018). Nanomaterial has many applications in various areas of petrol designing, such as investigation, boring, and creation (Mohamadian et al. 2018), because NPs have higher surface area-to-volume ratios compared with larger particles. This characteristic provides them with several advantages, including greater strength, improved electrical and thermal properties, and increased chemical reactivity (Godson et al. 2010); NPs added to the drilling fluid can help fill the gaps between particles and reduce the void space in the mudcake. This prevents fluid from flowing from the borehole into the formation. Various types of NPs, including ZnO, montmorillonite, carbon nanotubes, SiO_2, nanoclay, nanographite, TiO_2, Fe_2O_3, graphene, calcium oxide, CuO, and Al_2O_3, have been introduced into drilling fluid to improve fluid loss control and rheology (Al-saba et al. 2018).

Mohammed (2017) conducted a study to examine the impact of Fe_2O_3 NPs of two different sizes (3 nm and 30 nm) on the rheological and filtration properties of bentonite-based drilling fluids under HTHP conditions. The study found that the smaller NPs had a greater effect on increasing the PV and YP than the larger ones. In another study, researchers observed that by varying the concentration of silica NPs in the WBM from 0.001 wt% to 1.5 wt%, the viscosity of the drilling mud increased (Gbadamosi et al. 2019). Cheraghian et al. (2015) demonstrated that incorporating nanoclay into PAM had a beneficial impact on the viscosity characteristics of the polymer solution. In recent years, there has been a great interest in improving the stability of polymers through modification of their structure or by using NPs (Hu et al. 2017). To improve control over rheological properties and maintain thermal stability, the market has introduced activated weighting agents, thermally stable clay, and fluid systems with temperature and contaminant tolerance. These polymers provide filtration and rheological properties as well as high thermal stability. Ongoing research aims to identify the micromechanisms of rheology at high temperatures (Ezell and Harrison 2008). Fe_2O_3 NPs impart a positive charge to the bentonite-water suspension, thereby enhancing shear stresses at all shear rates (Rezaei et al. 2020). The use of NPs significantly improved the thermal stability of hydrolyzed PAM over a 12-day test period. In other words, the effective viscosity was approximately five times higher at a 0.8 wt% loading (Haruna et al. 2019). The studies conducted by Haruna et al. confirm that the dispersion formed by SMag-NPs-PAM showed higher viscosity and better mobility control. Additionally, it exhibited a lower contact angle and interfacial tension compared with pure SMag-NPs, PAM, and IO-NPs-PAM under high-temperature and high-salinity conditions (Fakher et al. 2020).

Two possible schemes have been proposed to explain the phenomenon of decreased viscosity. The first scheme involves the formation of carboxylic acid groups on the PAM backbone. This leads to a reaction with hydroxyl groups on the CQDs, resulting in the formation of ester bonds. The second scheme suggests that long macromolecular chains in the PAM are broken down into smaller chains. The CQDs can protonate the carboxylate groups in the PAM, converting them from –COO− to –COOH. This increases the acidity of the polymer and eventually causes a conformational transition, changing the polymer from a stretched state to a coiled state (Haruna et al. 2019).

Polymer injection is an enhanced oil recovery method that improves mobility control. It is used to increase oil recovery beyond what can be achieved through primary and secondary production mechanisms (Nourafkan et al. 2019). High-temperature, high-salinity, and extreme pH conditions can have a significant impact on the stability of polymers and degrade their performance in enhanced oil recovery (Caenn et al. 2011). The presence of MWCNTs significantly increased the viscosity of polymer solutions compared with pure co/terpolymer solutions (Geehan et al. 1989). In this study, we tested and quantified the sensing and rheological properties of drilling mud modified with nano-Fe_2O_3 at different temperatures. We used the shear stress vs. shear rate variation for analysis. The objective of measuring fluid control was to enhance the cost-effectiveness, safety, and profitability of drilling operations.

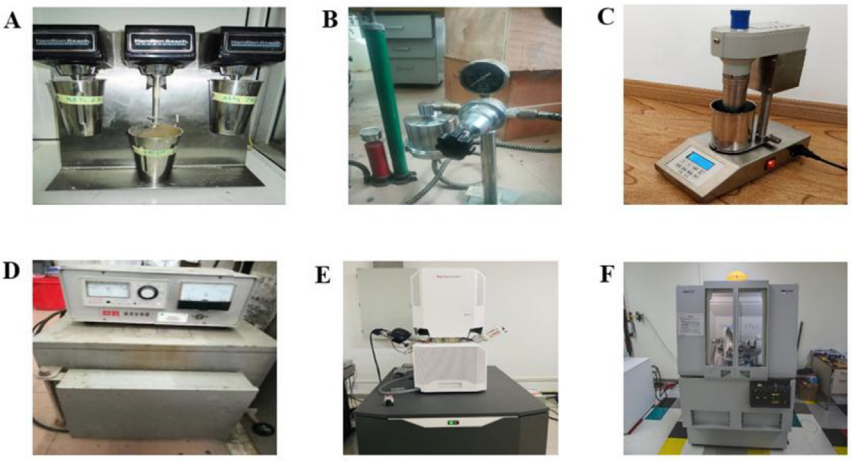

Fig. 1—Experiment machine tools. (A) Hamilton Beach mixer, (B) filtration loss tester, (C) six-speed viscometer, (D) Chinese brand kSW muffle furnace, (E) Thermo Scientific Apreo S, and (F) XPert PRO MPD X-ray diffractometer.

Experimental Apparatus Instruments

For our experiments, we utilized specific equipment to perform various tasks. We used a Hamilton Beach mixer to effectively mix the components, a filtration loss tester to accurately measure the filtration loss, a six-speed viscometer to calculate the rheological properties, a Chinese brand kSW muffle furnace for calcining the dry fluid sludge, a Thermo Scientific Apreo S scanning electron microscope to analyze the samples, and an XPert PRO MPD X-ray diffractometer to examine the X-ray diffraction (XRD) of the six mudcakes. **Fig. 1** displays the instruments that were utilized for our experiments.

Experimental Process

Bentonite is used extensively to control some characteristics of incoming fluids that are clear-cut, such as cuttings movement to the surface, piece oil, and applying hydrostatic tension in the wellbore (Al-Yasiri and Al-Sallami 2015). Bentonite's capacity to restrict, tighten, and constantly drain fluid enhances its control over fluid flow in permeable systems (Khalil and Mohamed Jan 2012). For this reason, we implanted 22.5 g of organophilic soil bentonite to improve uniformity throughout the graded chamber. We utilized organophilic bentonite to demonstrate significant thixotropic or aging behavior, which is utilized in various applications. This thixotropic behavior is connected to its physical properties, specifically swelling and delamination behavior, as well as heterogeneous charge behavior that impacts particle shape. We added 350 mL of fresh water to help decay the excess debris. Using an electric blender, we blended the contents in the bucket until there were no more projections. We added 0.5 wt%, 1 wt%, and 1.5 wt% NPs; 2 wt%, 2.5 wt%, and 3 wt% NPs after 16 hours of supporting the damaged fluid in suspension. The pursuit of consistent rheology is essential when selecting the rate and insertion of Fe_2O_3. By incorporating the specified quantity, we successfully achieved a desirable rheological constant. **Fig. 2** displays the assessment

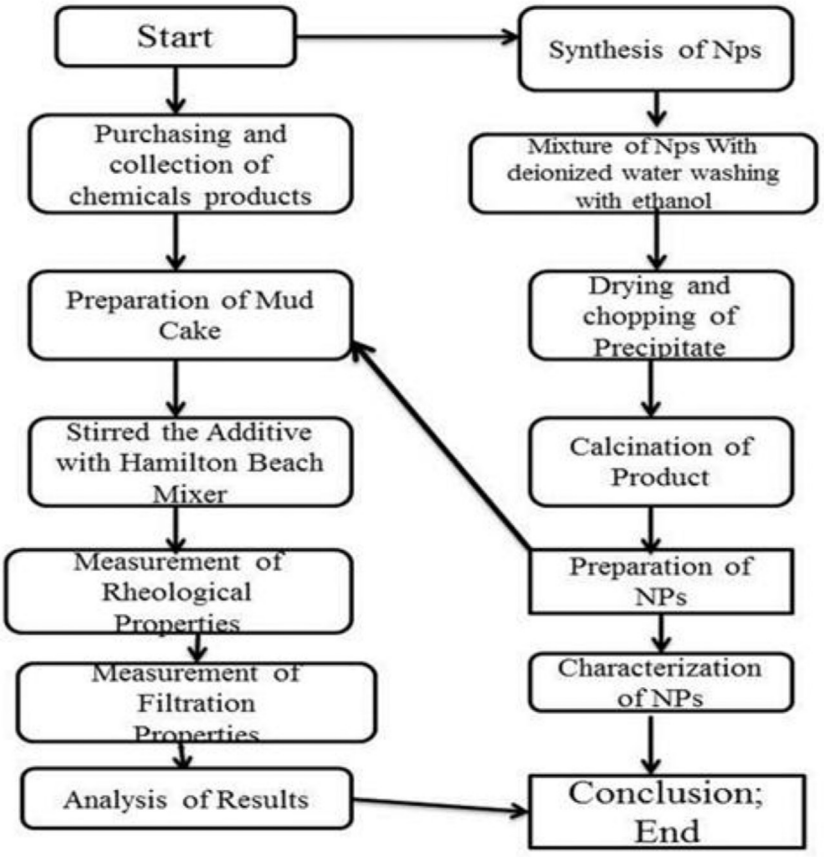

Fig. 2—Flow chart of experimental process.

" A = 0.5 wt.% NPs " "B = 1 wt. % NPs " " C = 1.5wt% NPs " " D = 2wt% NPs " " E =2.5wt% NPs " " F =3 wt.% NPs "

Fig. 3—Mudcake with different concentrations of Fe_2O_3 NPs.

affiliation following a 2-minute electric blender homogenization and persistent mixing of test fluids, while **Fig. 3** displays the six mudcakes made with varying concentrations of Fe_2O_3 NPs. The materials utilized in the underlying cycle should be visible in **Table 1**.

Constituent	Remark	Concentration
Fresh water	Based fluid	350 mL
Bentonite	Organophilic clay	23 g
Barite	Weighting agent	17 g
Carboxyl methyl cellulose	Fluid loss additive	2 g
Potassium chloride	Water activity and density	2.5 g
Anionic acrylic	Viscosity control agent	2.5 g
Caustic soda	pH control	0.6 g

Table 1—Mudcake formulation.

Synthesis of Fe_2O_3 NPs. The synthetic precipitation strategy was decided to incorporate Fe_2O_3 NPs. We degraded 5 g of ferric chloride hexahydrate ($FeCl_3 \cdot 6H_2O$) in 100 mL of demineralized water. The products were then cleaned and rinsed with ethanol and deionized water to eliminate the overflow base. It was dried in a hot air stove for 2 hours at 100°C after some time had passed. After that, the object was sliced into pieces, which were calcined for 4 hours at 450°C in a cover. Eventually, the XRD revealed the bronzed natural-hued hematite powder content, with the development we anticipated to complete the scanning electron microscopy (SEM).

Rheological Measurements. Rheological investigation plays a crucial role in the polymer-flooding process. To achieve the best possible oil recovery, it is important to accurately determine the viscosity of the polymer. This allows for a favorable mobility ratio between the oil and the displacing fluid. However, it is worth noting that the viscosity of the polymer can be affected by both the temperature and salinity of the oil reservoirs (Muller et al. 1980; Seright et al. 2010; Al-Sabagh et al. 2016). Temperature and salinity affect PAM viscosity differently. Higher temperature reduces viscosity by increasing polymer solubilization (Pramanik et al. 2017). Rheology is best explained as the study of deformation or flow behavior under applied stress (Temraz and Hassanien 2016). Many principles are affected by pipe sticking, which depends on the rheology of the drilling fluid (Shakib et al. 2016). Khalil et al. examined the viscoplastic lead of a liquid that penetrates biopolymers. The results demonstrated that the assortment technique can accurately predict the rheological response to these liquids' actions (Bourgoyne et al. 1986; Abduo et al. 2016). As a unit that demonstrates the thixotropic feature, the gel strength is expressed as heads or tails (Seright et al. 2010). Because of the strong particles' mechanical grinding, plastic thickness is also known as the liquid's mechanical obstruction (Bingham 1922). Yield strength, a limitation of Bingham's plastic model, is the crucial stream security attained by electrochemical reactions between mud particles that penetrate (Herschel and Bulkley 1926). Using the Bingham model, the rheological limits of all exhausting fluids, including plasticity and apparent consistency, yield strength, and gel strength, are still a mystery. The American Oil Foundation (programming connection point) utilized the accompanying conditions to decide the rheological limits, which included apparent viscosity, PV, and YP, as per the Bingham plastic model. The Bingham plastic model does not fully settle the sensible consistency, plastic thickness, or yield attestation.

Determination of Apparent Viscosity.

$$\mathrm{AV} = \frac{\tau}{\gamma} = \frac{5.1 \cdot L \cdot 00}{1020} \qquad P, \tag{1}$$

$$\mathrm{AV} = \frac{\tau}{\gamma} = \frac{5.1 \cdot L \cdot 00}{1020} \qquad P, \tag{2}$$

$$\mathrm{AV} = \frac{L600}{2} \qquad c, \tag{3}$$

where τ is the shear stress (Pa), $L600$ is the ofite reading at 600 rev/min, and 1020 s^{-1} is the shear speed corresponding to the reading at 600 rev/min.

Determination of PV. $\mathrm{PV} = tg\alpha = \dfrac{\tau 2010 - \tau 510}{\gamma 600 - \gamma 300}$. (4)

Determination of YP. From the Bingham plastic model, we have

$$\tau = \mathrm{PV} \cdot \gamma + \mathrm{YP} \geq \mathrm{YP} = \tau - \mathrm{PV} \cdot \gamma. \tag{5}$$

$$\mathrm{YP} = \mathrm{YP} = \tau - 1020\frac{\tau 1020 - \tau 510}{1020 - 510} \cdot 1020 = 0.511[L600 - 2(L600 - L300)] \tag{6}$$

$$\mathrm{YP} = 0.511 \cdot \left(2 \cdot L300 - L600\right) = 0.511\left[L300 - \left(L600 - L300\right)\right].$$

$$\mathrm{YP} = 0.511 \cdot \left(L300 - \mathrm{PV}\right). \tag{7}$$

$$\mathrm{YP} = \frac{0.511(L300 - \mathrm{PV})}{0.4788}, \tag{8}$$

and

$$1,067 \cdot (L300 - \mathrm{PV}) \sim \mathrm{YP} = L300\text{–}\mathrm{PV}\left[\frac{11\ \mathrm{lb}}{100\ \mathrm{ft}^2}\right], \tag{9}$$

where γ is the shear rate or strain rate. To find the shear stress (τ), do the following:

- For pascal, multiply the ofite readings by 0.511.
- For decapascal, multiply the ofite readings by 5.11.
- For millipascal, multiply the ofite readings by 511.
- For pounds per 100 square feet, multiply the readings by 1.067.

Standard Error. The limit of any explanatory laid out to facilitate the nonlinear backslide at a high shear rate will describe its accuracy. As this limit shifts with each logical articulation, the determined rheological boundaries offer unmistakable qualities for different models. The standard error for each rheological model has been determined utilizing Eq. 10 (Papanastasiou 1987). At last, the best-fitted and most successful demonstration was determined.

$$\text{Standard Error} = \frac{1,000 * \left[\frac{\sum(\text{measured value} - \text{calculated value})^{1/2}}{(\text{number of data points} - 2)}\right]}{(\text{Maximum measured value - Minimum measured value})}. \tag{10}$$

Results and Analysis

Characteristics of Fe_2O_3 NPs. ***XRD of Fe_2O_3 NPs.*** The powder XRD pattern of the synthesized Fe_2O_3 NPs is shown in **Fig. 4**. The XRD analysis of synthesized NPs demonstrates the characteristics pattern of α-Fe_2O_3. The characteristic peaks appear at the following 2θ ranges ≈24.15o, 33.760, 36.250, 42.340, 50.120, 54.20, 64.900, and 72.650, which correspond to 104.14, 307.85, 225.14, 68.57, 92.72, 110.57, 81.57, and 23.7. From the Debye-Scherrer formula $D = K\lambda\beta \cos\theta$, the crystal size of the synthesized iron NP was computed to be about 40 nm. From XRD analysis, the crystallinity of synthesized NPs was found to be 75.46%.

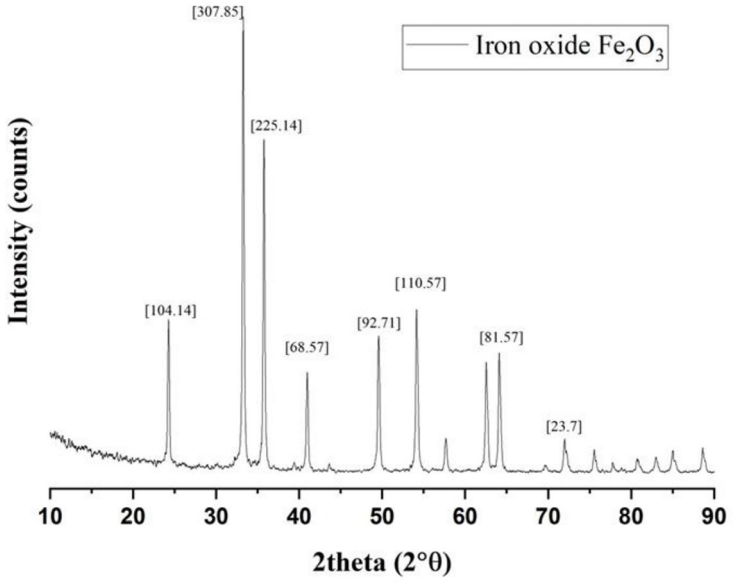

Fig. 4—XRD Fe_2O_3 NP analysis

Physical Description of Fe_2O_3 NPs. Fe_2O_3 NPs are composed of iron and oxygen atoms and are characterized by their distinct appearance and properties that differentiate them from bulk iron oxide materials. These NPs typically have diameters ranging from 1 nm to 100 nm, making them thousands of times smaller than a human hair. As a result of their small size, they exhibit unique properties and behaviors compared with their bulk counterparts. The physical description of Fe_2O_3 NPs emphasizes their small size, unique colors, and magnetic properties, which make them a fascinating and versatile material with numerous potential applications across various fields. In **Table 2**, we present the physical properties of the iron oxide used in our experiments, including a particle size of 30 nm, a specific surface area of 37 m^2/g, and a bulk density of 0.21 g/cm^3.

Properties	Typical Value
Purity	99.90%
Appearance	Red powder
Size	20–30 nm
Ash	>0.21 wt%

Table 2—Physical properties of Fe_2O_3 NPs.

SEM of Fe_2O_3 and Mudcake E. For the iron oxide SEM in **Fig. 5**, we used a small quantity of iron oxide already synthesized; with Thermo Scientific Apreo for SEM, to perform elemental analysis of the iron oxide, we have done the SEM under 5,000X. According to the SEM in **Fig. 6**, we notice that the grains are in the form of clusters of grains, where each grain is in the form of flowers in assembly. We can observe that the SEM of Mudcake E is characterized by large components in the form of bubbles, above all an advantage for the fluid loss control; a magna in assembly

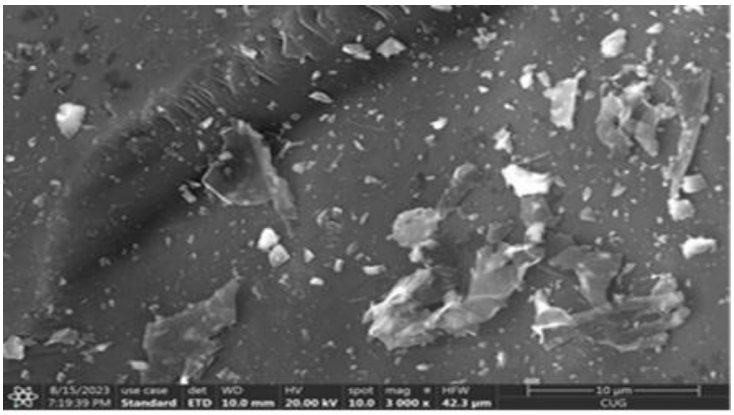

Fig. 5—SEM of Fe_2O_3.

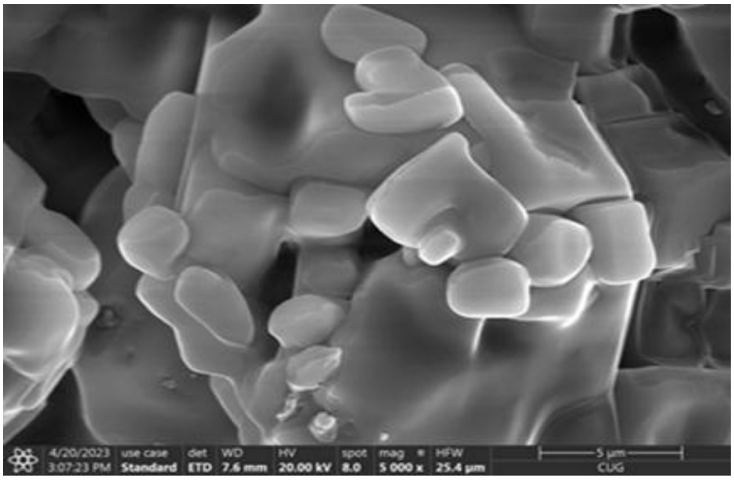

Fig. 6—SEM of Mudcake E.

Impact of Fe_2O_3 on the PV. In terms of how the Fe_2O_3 NPs affect the consistency of the plastic, we discovered that the number of NPs grows and shrinks in tandem with temperature and that the plastic thickness grows effectively. To bring rock shavings to the surface, the PV with NP fixation ascends and chips away at the liquid's entry restriction, especially in large apertures where the siphon's annular speed is relatively small (Casson 1959). This is the result of the solids rate increasing and the size of the important solid areas decreasing. According to assessments conducted by Yahia and Khayat (2001), the differentiation appears to be the particles or a combination of them, and the plastic's thickness is developing in light of the presence of NPs in WBM. The results showed a pattern. Mudcake A was inspected at 10,000 psi and a temperature of 300°F. As demonstrated in **Fig. 7** and **Table 3**, we discover a significant reduction of 88.10% of WBM PV, with an exceptionally low fraction of NPs about the nanoeffect on the plastic thickness of the WBM. Debris will be less flexible and more likely to stick behind the drill head and come out of the slurry, which will make drilling impossible. Nevertheless, with the addition of NP blends of 2.5 wt% and 3 wt% NPs, a reduction of 14.77% PV was seen at high temperatures of 300°F and pressures of 10,000 psi.

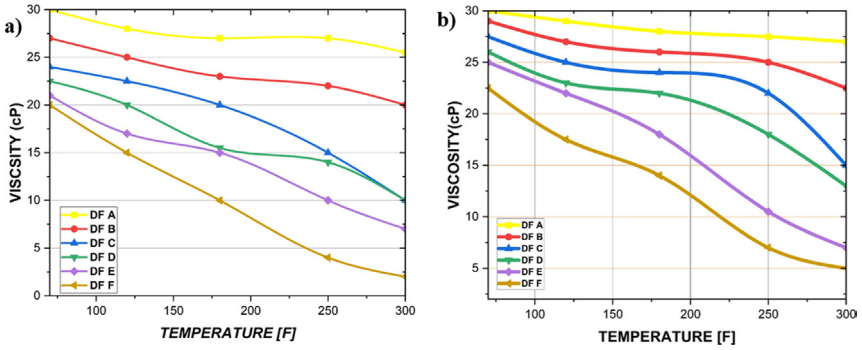

Fig. 7—(a) PV variations with NP and temperature of WBM. (b) YP variations.

Exceptionally high PV proportion can be reduced by ownership limit, extremely high consistency and syphon tension, the partition of flood solids, and incapacitating. There is a 2.7 YP-PV extent. It displays the drilling fluid's speed profile as it passes through the annulus, or space created between a drillpipe and the penetrated wall. A greater YP-PV extent results in a thicker profile, which is necessary for slurry to move cuttings clearance (Ahmad et al. 2017). In addition, a high (YP-PV) ratio or a low *n* value allows better cuttings transport and better hole cleaning (Samaei and Tahmasbi 2007).

	70°F	120°F	180°F	250°F	300°F
Mudcake A	30	28	27	27	25.5
Mudcake B	27	25	23	22	20
Mudcake C	24	22.5	20	15	10
Mudcake D	22.5	20	15.5	14	10
Mudcake E	21	17	15	10	7
Mudcake F	20	15	10	4	2

Table 3—PV variation under temperature and nano-Fe_2O_3.

Thermal Impact of Fe_2O_3 on the YP. The range of YP that affects iron oxide NPs under high strain and temperature circumstances is displayed in **Fig. 8b** and **Table 4**. The centralization of NPs causes a global decrease in temperature that is below the expectations of many. Changes in the liquid solids' surface properties, their centralization and electrical arrangement, and the kinds and fixation of particles in the liquid phase of the borehole as the association of NPs expands are the causes of these variations in yield strength.

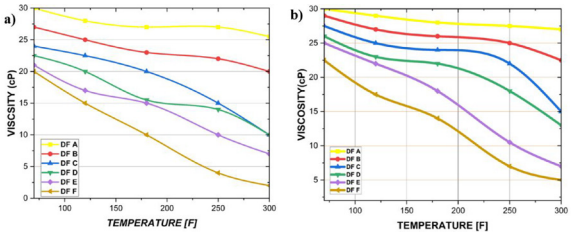

Fig. 8—(a) 10-second gel strength of WBM; (b) 10-minute gel strength of WBM.

	70°F	120°F	180°F	250°F	300°F
Mudcake A	30	29	28	27.5	27
Mudcake B	29	27	26	25	22.5
Mudcake C	27.5	25	24	22	15
Mudcake D	26	23	22	18	13
Mudcake E	25	22	18	10.5	7
Mudcake F	22.5	17.5	14	7	5

Table 4—YP variation under temperature and nano-Fe_2O_3.

Effect of Nano-Fe_2O_3 on Gel Strength Variation under HTHP. Tables 5 and 6 and **Figs. 8a and 8b** show that the iron oxide size is 0.5 wt%. At 300°F and 10,000 psi of strain, Mudcake A showed a significant decrease in WBM and YP of 76.60%. Drill cuttings are essentially affected in significant areas of strength by this reduction. The assessment of the impact of iron oxide NPs on the rheological properties of a WBM in a HTHP environment and the proper well restoration during crippling conditions (Okrajni and Azar 1986). Nonetheless, compared with thermally settled samples, the WBM increases by 2.5 wt%. Under comparable HTHP conditions, NPs only experience a 9.57% decrease in yield limit.

	70°F	120°F	180°F	250°F	300°F
Mudcake A	15	14	13	12.5	12.5
Mudcake B	14	13	12	10	8
Mudcake C	13	12.5	11	11	9.5
Mudcake D	11	9.5	9	8	7
Mudcake E	9	7	6	5	3
Mudcake F	8	5	3.5	3	2

Table 5—10-second gel strength variation under temperature and nano-Fe_2O_3.

	70°F	120°F	180°F	250°F	300°F
Mudcake A	13	13.5	14	15	16
Mudcake B	12	12	13	14	15
Mudcake C	11	12	13	13.5	15
Mudcake D	8	9	9.5	11	13
Mudcake E	4	6	7.5	9	11
Mudcake F	3	4	5	7	2

Table 6—10-minute gel strength under temperature and nano-Fe_2O_3.

Analyze Shear Stress vs. Shear Rate Variation under HTHP

The stream lead's sign indicates a liquid's propensity to shear when subjected to strain and temperature changes. Shear pressure analysis has demonstrated that as NP concentration increases, so does the liquid's growth due to shear (refer to **Figs. 9A through 9F**). Due to the high heat and strains, Mudcake A was subsequently reduced, and the garbage structure as a whole experienced a high-shear, low-fat mentality. In any case, as the concentration of NPs rises to the ideal combination of 2.5 wt% NPs, the liquid structure demonstrates its thermal stability. According to the results obtained (**Tables 7 through 12**), when the temperature increases, the shear stress vs. rate changes rapidly, we can deduce that the temperature and the pressure influence the shear stress vs. rate.

	70°F	120°F	180°F	250°F	300°F
$\tau_{1,400}$	69	50	35	15	10
$\tau_{1,200}$	48	35	25	11	9
$\tau_{1,000}$	40	30	20	10	8
τ_{800}	30	25	15	9	6
τ_{600}	25	20	10	8	5
τ_{400}	20	15	10	4	3
τ_{200}	10	10	9	0	0

Table 7—Shear stress vs. shear rate variation with temperature for Mudcake A.

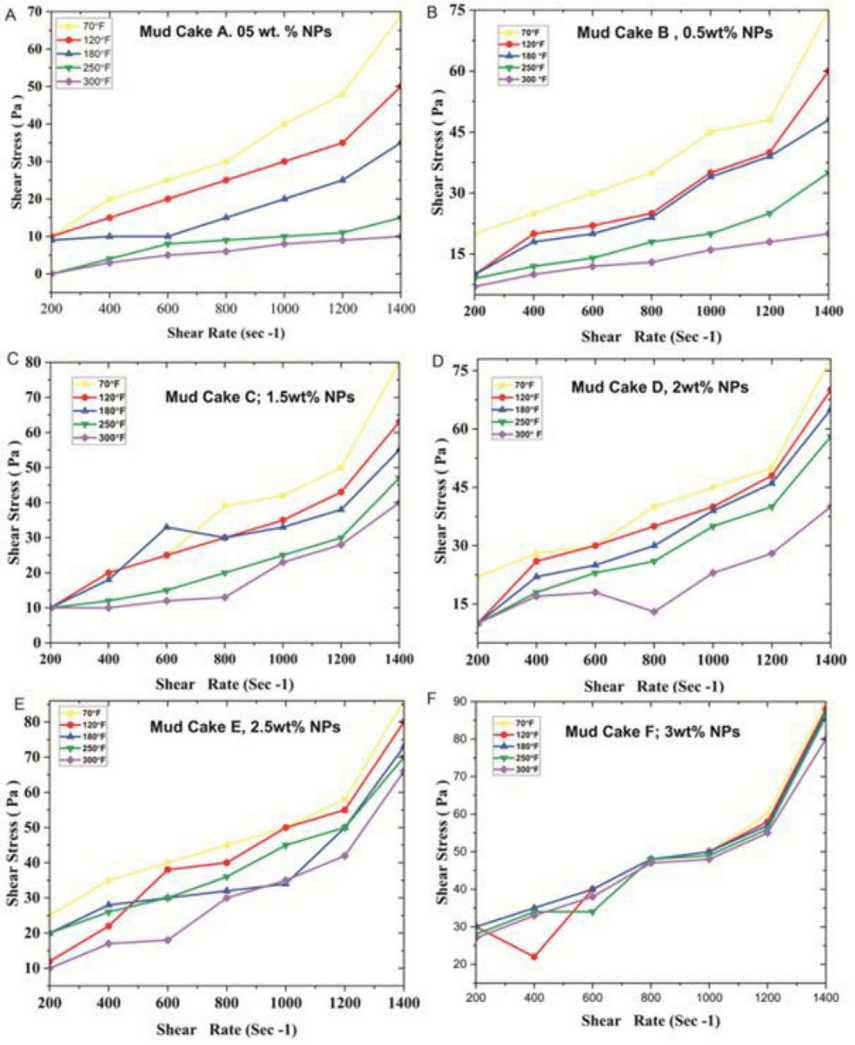

Fig. 9—Shear stress vs. shear rate variant with temperature for mudcakes (A, B, C, D, E, and F).

	70°F	120°F	180°F	250°F	300°F
$\tau_{1,400}$	75	60	48	35	20
$\tau_{1,200}$	48	40	39	25	18
$\tau_{1,000}$	45	35	34	20	16
τ_{800}	35	25	24	18	13
τ_{600}	30	22	20	14	12
τ_{400}	25	20	18	12	10
τ_{200}	20	10	10	9	7

Table 8—Shear stress vs. shear rate variation with temperature for Mudcake B.

	70°F	120°F	180°F	250°F	300°F
$\tau_{1,400}$	78	63	55	47	40
$\tau_{1,200}$	50	43	38	30	28
$\tau_{1,000}$	42	35	33	25	23
τ_{800}	39	30	30	20	13
τ_{600}	25	25	33	15	12
τ_{400}	20	20	18	12	10

	70°F	120°F	180°F	250°F	300°F
τ_{200}	10	10	10	10	10

Table 9—Shear stress vs. shear rate variation with temperature for Mudcake C.

	70°F	120°F	180°F	250°F	300°F
$\tau_{1,400}$	80	70	65	58	40
$\tau_{1,200}$	50	48	46	40	28
$\tau_{1,000}$	45	40	39	35	23
τ_{800}	40	35	30	26	13
τ_{600}	30	30	25	23	18
τ_{400}	28	26	22	18	17
τ_{200}	22	10	10	10	10

Table 10—Shear stress vs. shear rate variation with temperature for Mudcake D.

	70°F	120°F	180°F	250°F	300°F
$\tau_{1,400}$	86	80	73	70	66
$\tau_{1,200}$	58	55	50	50	42
$\tau_{1,000}$	50	50	34	45	35
τ_{800}	45	40	32	36	30
τ_{600}	40	38	30	30	18
τ_{400}	35	22	28	26	17
τ_{200}	25	12	20	20	10

Table 11—Shear stress vs. shear rate variation with temperature for Mudcake E.

	70°F	120°F	180°F	250°F	300°F
$\tau_{1,400}$	90	88	87	86	80
$\tau_{1,200}$	60	58	57	56	55
$\tau_{1,000}$	50	50	50	49	48
τ_{800}	48	48	48	48	47
τ_{600}	40	40	40	34	38
τ_{400}	35	22	35	34	33
τ_{200}	30	30	30	28	27

Table 12—Shear stress vs. shear rate variation with temperature for Mudcake F.

Effect of Nano-Fe_2O_3 on the Rheology Behavior of Drilling Muds

The estimation of the rheology of drilling muds of the Dibela oil field exhibits the shear diminishing way of behaving which demonstrates the expansion in shear rate causes a decrease in consistency, as displayed in **Fig. 10**. According to **Fig. 10**, the PV initially remains unchanged at a low concentration of NP. However, at higher concentrations, the PV improves. Specifically, Mudcake B with a concentration of 1 wt% shows a 10% improvement in PV compared with Mudcake A at 0.5 wt%. Additionally, Mudcake F with 3 wt% NP demonstrates an approximately 30% increase in PV. The increase in PV can be attributed to the presence of NPs, which contribute to the overall dispersed solids in the sludge system. A low shear rate builds the iron oxide NP focus and shows higher consistency contrasted with low NP rate mud; it uncovers a significant property of the penetrating liquid as high viscosities are fundamental in static circumstances and low viscosities in conditions to eliminate cuttings from the lower part of the opening (Anawe et al. 2014).

Effect of Nano-Fe_2O_3 on API Fluid Loss

The impact of nano-Fe_2O_3 concentrations on fluid loss is illustrated in **Fig. 11**. For all NP concentrations, the API fluid loss is reduced compared with the base mud, demonstrating the significant capability of NPs to control fluid loss. In the case of the base mud, Mudcake

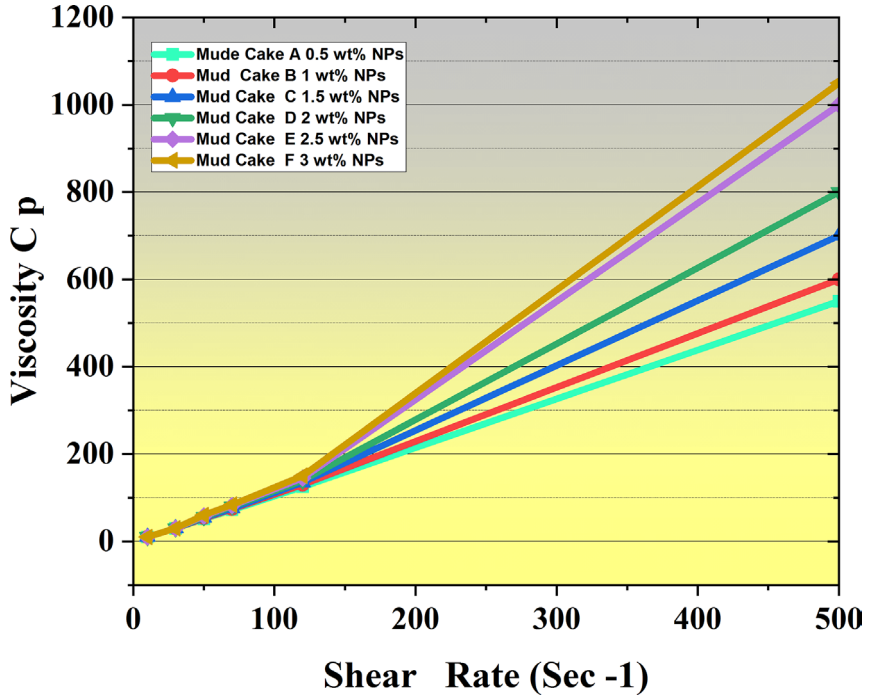

Fig. 10—Effect of iron oxide NP on viscosity at different shear rates.

A yields 6 mL of filtrate in the 30-minute API filter test. On the other hand, Mudcake B with an NP concentration of 1 wt% produces 5.3 mL of filtrate, representing a 12.4% improvement in fluid loss control compared with Mudcake A. Experimental observation reveals that the cumulative fluid loss is minimized (5.3 mL) at an NP concentration of 1 wt%. At higher NP concentrations, the cumulative fluid losses are slightly higher (6–4.5 mL), confirming the optimal performance of hematite NPs at a concentration of 2.5 wt%. This value aligns closely with the findings of previous experimental work. In conclusion, it can be inferred that a concentration of 2.5 wt% provides a sufficient quantity of NPs to block the pore space of the filter paper. At higher concentrations, the volume of NPs relative to other additives increases, which affects the formation of a proper bridge and results in a slight increase in filtrate volume.

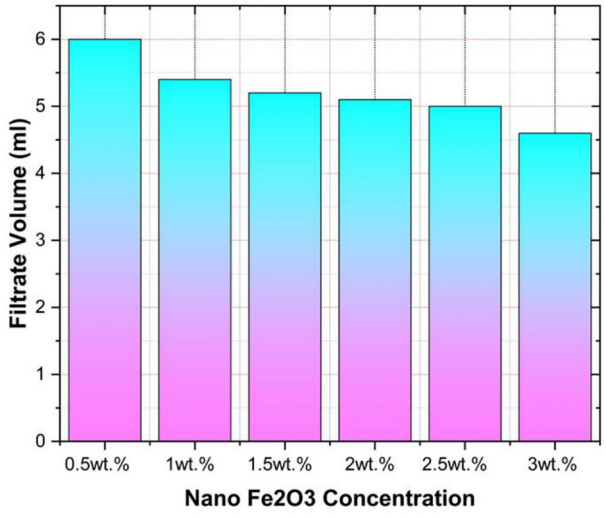

Fig. 11—Comparison of total fluid loss between drilling muds after 30 minutes.

Conclusion

Based on the comprehensive analyses conducted on iron oxide solutions, several key conclusions can be drawn:

1. Impact of iron oxide under HTHP conditions: The addition of iron oxide to drilling fluids under HTHP conditions leads to increases in PV, YP, and gel strength. However, these increases remain within acceptable ranges for optimal performance of WBDF.
2. Optimal concentration of iron NPs: A concentration of 2.5 wt% iron NPs proves to be effective in maintaining highly and thermally stable rheological properties under extreme conditions of 300°F temperature and 10,000 psi pressure. Despite a slight decrease in gel strength, Mudcake E, containing 2.5 wt% NPs, retains a high YP-PV ratio of 2.7 even after 16 hours of hot rolling.

3. Role of hematite Fe_2O_3: Hematite Fe_2O_3 plays a crucial role in achieving a liquid design that balances viscosity without being excessively restrictive or thick at elevated temperatures. It effectively regulates the consistency collection speed with changes in shear rate, providing stability to the drilling fluid under HTHP conditions.
4. Effect on filter-cake thickness and fluid loss: Increasing concentrations of iron oxide NPs result in decreased thickness of the filter cake and fluid loss. Rheological testing and SEM analysis of Mudcake E containing 2.5 wt% iron oxide demonstrate satisfactory rheological properties and liquid loss characteristics. Moreover, when combined with anionic acrylic as a loss circulation material, this formulation exhibits excellent stability and sealing capabilities at high temperatures, making it suitable for challenging HTHP wells prone to circulation loss.
5. Effectiveness at lower concentrations: Even at a concentration of 1 wt%, iron oxide NPs significantly reduce fluid loss and mudcake thickness compared with formulations without iron oxide. Mud formulations with slightly higher concentrations continue to perform optimally, indicating the effectiveness of iron oxide NPs in controlling fluid loss and maintaining rheological stability across various concentrations.

References

Aadnoy, B. S. and Chenevert, M. E. 1987. Stability of Highly Inclined Boreholes. *SPE Drilling Eng* **2** (04): 364–374. https://doi.org/10.2118/16052-PA.

Abdo, J. and Haneef, M. D. 2013. Clay Nanoparticles Modified Drilling Fluids for Drilling of Deep Hydrocarbon Wells. *Appl Clay Sci* **86**: 76–82. https://doi.org/10.1016/j.clay.2013.10.017.

Abdo, J. and Haneef, M. D. 2012. Nano-Enhanced Drilling Fluids: Pioneering Approach to Overcome Uncompromising Drilling Problems. *J Energy Resour Technol* **134** (1): 1. https://doi.org/10.1115/1.4005244.

Abdo, J., Zaier, R., Hassan, E. et al. 2014. ZnO-Clay Nanocomposites forenhancedrillingatHTHPconditions. *Surf Interface Anal* **46** (10–11): 970–974. https://doi.org/10.1002/sia.5454http://onlinelibrary.wiley.com/doi/10.1002/sia.5454/abstract.

Abduo, M. I., Dahab, A. S., Abuseda, H. et al. 2016. Comparative Study of Using Water-Based Mud Containing Multiwall Carbon Nanotubes versus Oil-Based Mud in HPHT Fields. *Egypt J Petrol* **25** (4): 459–464. https://doi.org/10.1016/j.ejpe.2015.10.008.

Ahmad, H. M., Kamal, M. S., Murtaza, M. et al. 2017. Improving the Drilling Fluid Properties Using Nanoparticles and Water-Soluble Polymers. Paper presented at the SPE Kingdom of Saudi Arabia Annual Technical Symposium and Exhibition, Dammam, Saudi Arabia, 24−27 April. https://doi.org/10.2118/188140-MS.

Akhtarmanesh, S., Shahrabi, M. J. A., and Atashnezhad, A. 2013. Improvement of Wellbore Stability in Shale Using Nanoparticles. *J Pet Sci Eng* **112**: 290–295. https://doi.org/10.1016/j.petrol.2013.11.017.

Al-saba, M. T., Al Fadhli, A. ., Marafi, A. . et al. 2018. Application of Nanoparticles in Improving Rheological Properties of Water Based Drilling Fluids. Paper presented at the SPE Kingdom of Saudi Arabia Annual Technical Symposium and Exhibition, Dammam, Saudi Arabia, 23−26 April. https://doi.org/10.2118/192239-MS.

Al-Sabagh, A. M., Kandile, N. G., El-Ghazawy, R. A. et al. 2016. Solution Properties of Hydrophobically Modified Polyacrylamides and Their Potential Use for Polymer Flooding Application. *Egypt J Petrol* **25** (4): 433–444. https://doi.org/10.1016/j.ejpe.2015.03.014.

Al-Yasiri, M. S. and Al-Sallami, W. T. 2015. How the Drilling Fluids Can Be Made More Efficient by Using Nanomaterials. *Am J Nano Res Appl* **3** (3): 41–45.

Anawe, P. A. L., Efeovbokhan, V. E., and Ayoola, A. A. 2014. Investigating Alternatives to Diesel in Oil-Based Drilling Mud Formulations Used in the Oil Industry. *J Environ Earth Sci* **4** (14): 70–77.

Aramendiz, J. and Imqam, A. 2019. Water-Based Drilling Fluid Formulation Using Silica and Graphene Nanoparticles for Unconventional Shale Applications. *J Pet Sci Eng* **179**: 742–749. https://doi.org/10.1016/j.petrol.2019.04.085.

Baba Hamed, S. and Belhadri, M. 2009. Rheological Properties of Biopolymers Drilling Fluids. *J Pet Sci Eng* **67** (3–4): 84–90. https://doi.org/10.1016/j.petrol.2009.04.001.

Bayat, A. E. and Shams, R. 2019. Appraising the Impacts of SiO2, ZnO and TiO2 Nanoparticles on Rheological Properties and Shale Inhibition of Water-Based Drilling Muds. *Colloids Surf A: Physicochem Eng Aspects* **581**: 123792. https://doi.org/10.1016/j.colsurfa.2019.123792.

Bingham, E. C. 1922. *Fluidity and Plasticity*. New York, New York, USA: McGraw-Hill Book Company.

Bourgoyne, A. T., Millheim, K. K., Chenevert, M. E. et al. 1986. *Applied Drilling Engineering*. Richardson, Texas, USA: Society of Petroleum Engineers.

Brady, J. F. and Brady, J. F. 1983. The Einstein Viscosity Correction in Dimensions. *Int J Multiphase Flow* **10** (1): 113–114. https://doi.org/10.1016/0301-9322(83)90064-2.

Caenn, R., Darley, H. C. H., and Gray, G. R. 2011. *Composition and Properties of Drilling and Completion Fluids*. Houston, Texas, USA: Gulf Professional Publishing.

Casson, N. 1959. *A Flow Equation for Pigment-Oil Suspensions of the Printing Ink Type*. Oxford, UK: Pergamon Press.

Cheraghian, G., Khalili Nezhad, S. S., Kamari, M. et al. 2015. Effect of Nanoclay on Improved Rheology Properties of Polyacrylamide Solutions Used in Enhanced Oil Recovery. *J Petrol Explor Prod Technol* **5** (2): 189–196. https://doi.org/10.1007/s13202-014-0125-y.

Christiansen, C. 1991. From Oil-Based Mud to Water-Based Mud. Paper presented at the SPE Health, Safety and Environment in Oil and Gas Exploration and Production Conference, The Hague, The Netherlands, 11−14 November. https://doi.org/10.2118/23359-MS.

Coussot, P., Bertrand, F., and Herzhaft, B. 2004. Rheological Behavior of Drilling Muds, Characterization Using MRI Visualization. *Oil & Gas Sci Technol - Rev IFP* **59** (1): 23–29. https://doi.org/10.2516/ogst:2004003.

Du, S., Wu, J., AlShareedah, O. et al. 2019. Nanotechnology in Cement-Based Materials: A Review of Durability, Modeling, and Advanced Characterization. *Nanomater (Basel)* **9** (9). https://doi.org/10.3390/nano9091213.

Esmaeili, A., Patel, R. B., and Singh, B. P. 2011. Applications of Nanotechnology in Oil and Gas Industry. *AIP Conf Proc* **1414**: 133–136. https://doi.org/10.1063/1.3669944.

Ezell, R. and Harrison, D. J. 2008. Design of Improved High-Density, Thermally-Stable Drill-In Fluid for HTHP Applications. Paper presented at the SPE Annual Technical Conference and Exhibition, Denver, Colorado, USA, 21−24 September. https://doi.org/10.2118/115537-MS.

Fakher, S., Ahdaya, M., and Imqam, A. 2020. Hydrolyzed Polyacrylamide – Fly Ash Reinforced Polymer for Chemical Enhanced Oil Recovery: Part 1 – Injectivity Experiments. *Fuel (Lond)* **260**: 116310. https://doi.org/10.1016/j.fuel.2019.116310.

Gbadamosi, A. O., Junin, R., Manan, M. A. et al. 2019. Synergistic Application of Aluminium Oxide Nanoparticles and Oilfield Polyacrylamide for Enhanced Oil Recovery. *J Pet Sci Eng* **182**: 106345. https://doi.org/10.1016/j.petrol.2019.106345.

Geehan, T., Dudleson, W. J., Boyington, W. H. et al. 1989. Incentive Approach to Drill Fluids Management: An Experience in Central North Sea. Paper presented at the SPE/IADC Drilling Conference, New Orleans, Louisiana, USA, 28 February−3 March. https://doi.org/10.2523/18639-MS.

Godson, L., Raja, B., Mohan Lal, D. et al. 2010. Enhancement of Heat Transfer Using Nanofluids—An Overview. *Renew Sustain Energy Rev* **14** (2): 629–641. https://doi.org/10.1016/j.rser.2009.10.004.

Haruna, M. A., Nourafkan, E., Hu, Z. et al. 2019. Improved Polymer Flooding in Harsh Environments by Free-Radical Polymerization and the Use of Nanomaterials. *Eng Fuels* **33** (2): 1637–1648. https://doi.org/10.1021/acs.energyfuels.8b02763.

Herschel, W. and Bulkley, R. 1926. Measurement of Consistency as Applied to Rubber-Benzene Solutions. *Am Soc Test Proc*: 621–633.

Hu, Z., Haruna, M., Gao, H. et al. 2017. Rheological Properties of Partially Hydrolyzed Polyacrylamide Seeded by Nanoparticles. *Ind. Eng. Chem. Res* **56** (12): 3456–3463. https://doi.org/10.1021/acs.iecr.6b05036.

Ismail, A. R., Aftab, A., Ibupoto, Z. H. et al. 2016. The Novel Approach for the Enhancement of Rheological Properties of Water-Based Drilling Fluids by Using Multi-Walled Carbon Nanotube, Nanosilica and Glass Beads. *J Pet Sci Eng* **139**: 264–275. https://doi.org/10.1016/j.petrol.2016.01.036.

Jain, R., Mahto, V., and Sharma, V. P. 2015. Evaluation of Polyacrylamide-Grafted-Polyethylene Glycol/Silica Nanocomposite as Potential Additive in Water Based Drilling Mud for Reactive Shale Formation. *J Nat Gas Sci Eng* **26**: 526–537. https://doi.org/10.1016/j.jngse.2015.06.051.

Khalil, M. and Mohamed Jan, B. 2012. Herschel-Bulkley Rheological Parameters of a Novel Environmentally Friendly Lightweight Biopolymer Drilling Fluid from Xanthan Gum and Starch. *J Appl Polym Sci* **124** (1): 595–606. https://doi.org/10.1002/app.35004.

Khodja, M., Canselier, J. P., Bergaya, F. et al. 2010. Shale Problems and Water-Based Drilling Fluid Optimisation in the Hassi Messaoud Algerian Oil Field. *Appl Clay Sci* **49** (4): 383–393. https://doi.org/10.1016/j.clay.2010.06.008.

Khoshakhlagh, A., Nazari, A., and Khalaj, G. 2012. Effects of Fe2O3 Nanoparticles on Water Permeability and Strength Assessments of High Strength Self-Compacting Concrete. *J Mater Sci Technol* **28** (1): 73–82. https://doi.org/10.1016/S1005-0302(12)60026-7.

László, K., Tombácz, E., and Josepovits, K. 2001. Effect of Activation on the Surface Chemistry of Carbons from Polymer Precursors. *Carbon* **39** (8): 1217–1228. https://doi.org/10.1016/S0008-6223(00)00245-1.

Le Guen, Y., Le Gouevec, J., Chammas, R. et al. 2009. CO2 Storage: Managing the Risk Associated With Well Leakage Over Long Time Scales. *SPE Proj Facil Constr* **4** (3): 87–96. https://doi.org/10.2118/116424-PA.

Li, X., Jiang, G., Yang, L. et al. 2019. Application of Gelatin Quaternary Ammonium Salt as an Environmentally Friendly Shale Inhibitor for Water-Based Drilling Fluids. *Eng Fuels* **33** (9): 9342–9350. https://doi.org/10.1021/acs.energyfuels.9b01798.

Livescu, S. 2012. Mathematical Modeling of Thixotropic Drilling Mud and Crude Oil Flow in Wells and Pipelines—A Review. *J Pet Sci Eng* **98–99**: 174–184. https://doi.org/10.1016/j.petrol.2012.04.026.

Mady, A., Mahmoud, O., and Dahab, A. S. 2020. Nanoparticle-Based Drilling Fluids as Promising Solutions to Enhance Drilling Performance in Egyptian Oil and Gas Fields. *Int J Ind Sustain Dev* **1** (1): 24–38. https://doi.org/10.21608/ijisd.2020.73471.

Mahmoud, M., Mohamed, A., Kamal, M. S. et al. 2019. Upgrading Calcium Bentonite to Sodium Bentonite Using Seawater and Soda Ash. *Eng Fuels* **33** (11): 10888–10894. https://doi.org/10.1021/acs.energyfuels.9b02900.

Ma, L., Luo, P., He, Y. et al. 2020. Improving the Stability of Multi-Walled Carbon Nano-Tubes in Extremely Environments: Applications as Nano-Plugging Additives in Drilling Fluids. *J Nat Gas Sci Eng* **74**: 103082. https://doi.org/10.1016/j.jngse.2019.103082.

Mao, H., Qiu, Z., Shen, Z. et al. 2015. Hydrophobic Associated Polymer Based Silica Nanoparticles Composite with Core–Shell Structure as a Filtrate Reducer for Drilling Fluid at Utra-High Temperature. *J Pet Sci Eng* **129**: 1–14. https://doi.org/10.1016/j.petrol.2015.03.003.

Mohamadian, N., Ghorbani, H., Wood, D. A. et al. 2018. Rheological and FIltration Characteristics of Drilling FLuids Enhanced by Nanoparticles with Selected Additives: An Experimental Study. *Adv Geo-Energy Res* **2** (3): 228–236. https://doi.org/10.26804/ager.2018.03.01.

Mohammed, A. S. 2017. Effect of Temperature on the Rheological Properties with Shear Stress Limit of Iron Oxide Nanoparticle Modified Bentonite Drilling Muds. *Egypt J Petrol* **26** (3): 791–802. https://doi.org/10.1016/j.ejpe.2016.10.018.

Muller, G., Fenyo, J. C., and Selegny, E. 1980. High Molecular Weight Hydrolyzed Polyacrylamides. III. Effect of Temperature on Chemical Stability. *J Appl Polym Sci* **25** (4): 627–633. https://doi.org/10.1002/app.1980.070250409.

Nagre, R. D., Zhao, L., and Owusu, P. A. 2014. Thermosaline Resistant Acrylamide-Based Polyelectrolyte as Filtration Control Additive in Aqueous-Based Mud. *Pet Coal* **56** (3): 222–230.

Nasser, J., Jesil, A., Mohiuddin, T. et al. 2013. Experimental Investigation of Drilling Fluid Performance as Nanoparticles. *World J Nano Sci Eng* **03** (3): 57–61. https://doi.org/10.4236/wjnse.2013.33008.

Nelson, E. B., Baret, J. F., and Michaux, M. 1990. 3 Cement Additives and Mechanisms of Action. *Dev Pet Sci.* **28**: 3-1–3-7. https://doi.org/10.1016/S0376-7361(09)70301-2.

Nourafkan, E., Haruna, M. A., Gardy, J. et al. 2019. Improved Rheological Properties and Stability of Multiwalled Carbon Nanotubes/Polymer in Harsh Environment. *J Appl Polym Sci* **136** (11): 47205. https://doi.org/10.1002/app.47205.

Okrajni, S. S. and Azar, J. J. 1986. The Effects of Mud Rheology on Annular Hole Cleaning in Directional Wells. *SPE Drilling Eng* **1** (4): 297–308. https://doi.org/10.2118/14178-PA.

Papanastasiou, T. C. 1987. Flows of Materials with Yield. *J Rheol* **31** (5): 385–404. https://doi.org/10.1122/1.549926.

Pramanik, C., Gissinger, J. R., Kumar, S. et al. 2017. Carbon Nanotube Dispersion in Solvents and Polymer Solutions: Mechanisms, Assembly, and Preferences. *ACS Nano* **11** (12): 12805–12816. https://doi.org/10.1021/acsnano.7b07684.

Rana, A., Arfaj, M. K., Yami, A. S. et al. 2020. Cetyltrimethylammonium Modified Graphene as a Clean Swelling Inhibitor in Water-Based Oil-Well Drilling Mud. *J Environ Chem Eng* **8** (4): 103802. https://doi.org/10.1016/j.jece.2020.103802.

Rashad, A. M. 2013. Metakaolin as Cementitious Material: History, Scours, Production and Composition – A Comprehensive Overview. *Constr Build Mater* **41**: 303–318. https://doi.org/10.1016/j.conbuildmat.2012.12.001.

Rezaei, A., Nooripoor, V., and Shahbazi, K. 2020. Applicability of Fe3O4 Nanoparticles for Improving Rheological and Filtration Properties of Bentonite-Water Drilling Fluids in the Presence of Sodium, Calcium, and Magnesium Chlorides. *J Petrol Explor Prod Technol* **10** (6): 2453–2464. https://doi.org/10.1007/s13202-020-00920-6.

Riley, M., Stamatakis, E., Young, S. et al. 2012. Wellbore Stability in Unconventional Shale - The Design of a Nano-Particle Fluid. Paper presented at the SPE Oil and Gas India Conference and Exhibition, Mumbai, India, 28−30 March. https://doi.org/10.2118/153729-MS.

Rodrigues, J. d., Lachter, E. R., deS, C. H. et al. 2006. New Multifunctional Polymeric Additives for Water-Based Muds. Paper presented at the SPE Annual Technical Conference and Exhibition, San Antonio, Texas, USA, 24−27 September. https://doi.org/10.2118/106527-STU.

Sadeghalvaad, M. and Sabbaghi, S. 2015. The Effect of the TiO2/Polyacrylamide Nanocomposite on Water-Based Drilling Fluid Properties. *Powder Technol* **272**: 113–119. https://doi.org/10.1016/j.powtec.2014.11.032.

Samaei, S. M. and Tahmasbi, K. 2007. The Possibility of Replacing Oil-Based Mud With the Environmentally Acceptable Water-Based Glycol Drilling Mud for the Iranian Fields. Paper presented at the E&P Environmental and Safety Conference, Galveston, Texas, USA, 5−7 March. https://doi.org/10.2118/106419-MS.

Seright, R. S., Campbell, A. R., Mozley, P. S. et al. 2010. Stability of Partially Hydrolyzed Polyacrylamides at Elevated Temperatures in the Absence of Divalent Cations. *SPE J.* **15** (02): 341–348. https://doi.org/10.2118/121460-PA.

Shakib, J. T., Kanani, V., and Pourafshary, P. 2016. Nano-Clays as Additives for Controlling Filtration Properties of Water–Bentonite Suspensions. *J Pet Sci Eng* **138**: 257–264. https://doi.org/10.1016/j.petrol.2015.11.018.

Sikora, P., Abd Elrahman, M., and Stephan, D. 2018. The Influence of Nanomaterials on the Thermal Resistance of Cement-Based Composites-A Review. *Nanomater (Basel)* **8** (7). https://doi.org/10.3390/nano8070465.

Singh, L. P., Agarwal, S. K., Bhattacharyya, S. K. et al. 2011. Preparation of Silica Nanoparticles and Its Beneficial Role in Cementitious Materials. *Nanomater Nanotechnol* **1**: 9. https://doi.org/10.5772/50950.

Taraghikhah, S., Kalhor Mohammadi, M., and Tahmasbi Nowtaraki, K. 2015. Multifunctional Nanoadditive in Water Based Drilling Fluid for Improving Shale Stability. Paper presented at the International Petroleum Technology Conference, Doha, Qatar, 6−9 December. https://doi.org/10.2523/IPTC-18323-MS.

Tehrani, A., Gerrard, D., Young, S. et al. 2009. Environmentally Friendly Water-Based Fluid for HPHT Drilling. Paper presented at the SPE International Symposium on Oilfield Chemistry, The Woodlands, Texas, USA, 20−22 April. https://doi.org/10.2118/121783-MS.

Temraz, M. G. and Hassanien, I. 2016. Mineralogy and Rheological Properties of Some Egyptian Bentonite for Drilling Fluids. *J Nat Gas Sci Eng* **31**: 791–799. https://doi.org/10.1016/j.jngse.2016.03.072.

Vermolen, E. C., van Haasterecht, M. J., Masalmeh, S. K. et al. 2011. Pushing the Envelope for Polymer Flooding Towards High-Temperature and High-Salinity Reservoirs with Polyacrylamide Based Ter-Polymers. Paper presented at the SPE Middle East Oil and Gas Show and Conference, Manama, Bahrain, 25−28 September. https://doi.org/10.2118/141497-MS.

Yahia, A. and Khayat, K. H. 2001. Analytical Models for Estimating Yield Stress of High-Performance Pseudoplastic Grout. *Cem Concr Res* **31** (5): 731–738. https://doi.org/10.1016/S0008-8846(01)00476-8.